E2F7 and E2F8 Play a Critical Role in Regulating Cell Cycle Progression

A Senior Honors Thesis

Presented in partial fulfillment of the requirements for graduation with distinction in

Molecular Genetics in the College of Biological Sciences

By

Grant Comstock

The Ohio State University

June 2009

Project Advisor: Dr. Gustavo Leone, Department of Molecular Immunology, Virology, and Medical Genetics

Abstract

E2f7 and *E2f8* are the most recently discovered members of the E2f family of transcription factors. The conventional knockout of either *E2f7* or *E2f8* in mice results in no observable phenotype. However, the concomitant loss of both genes results in massive apoptosis and dilation of blood vessels in the embryo and abnormal clustering of trophoblast cells in the placenta, leading to embryonic lethality at day 11.5 (E11.5). This indicated that the E2F7 and E2F8 proteins are functionally redundant and critical for embryonic viability at mid-gestation. Until recently however, the tissues, cellular processes, and molecular pathways regulated by these two proteins remained unknown. Here, we use a conditional knockout strategy to show that the extra-embryonic functions of E2F7 and E2F8 are both necessary and sufficient for embryonic viability at mid-gestation. Furthermore, we have defined a role for E2F7 and E2F8 in controlling the G_1/S transition. This led us to the discovery of an important genetic interaction between E2F7/E2F8 and E2F3a, critical for regulating the G1/S transition and maintaining embryonic viability. In summary, we identified a novel transcriptional network shared by E2F3a, E2F7 and E2F8 that is critical for control of cell proliferation, placental development and fetal viability.

Introduction

In response to an external growth stimulus, most cells will initiate a signaling cascade that will result in a proper and ordered cell cycle, culminating in the division of one cell into two identical daughter cells. A critical step in the entry into an active cell cycle involves the downregulation of Cyclin dependant kinase (Cdk) inhibitors, the induction of G_1 Cyclins, and the resulting association between Cyclins and their catalytic subunits (Murray, 2004; Sánchez and Dynlacht, 2005). These events eventually lead to the activation of Cdk complexes and the phosphorylation of Retinoblastoma (Rb) and its associated pocket protein family members p107 and p130. This phosphorylation results in the dissociation of pocket protein-E2f repressor complexes to promote E2f dependent transcription and the activation of E2f-dependent genes (Frolov and Dyson, 2004). Accumulation of E2f-dependent gene activity in late G_1 is believed to represent the final step in CDK-dependent signaling that irreversibly commits the cell to begin DNA replication. The high level of E2f-dependent transcription is then cut off in late S phase by a second wave of E2f-mediated repression that marks the end of DNA replication and pushes the cell into G_2. Therefore, through sequential waves of G0-repression, G_1-S activation and S-G_2 repression, the E2f family of transcription factors is able to orchestrate proper progression through the cell cycle.

The mammalian E2f family consists of eight genes (E2F1-8) (Figure 1). Structure-function studies classify these eight genes are divided into an activator subclass and a repressor subclass. E2F1, E2F2, and E2F3a make up the activator subclass, due to their strong transcription activation domains, with an Rb binding site buried within this region (Cam and Dynlacht, 2003). During G_0, the activation domain is held inactive by

the binding of Rb in this region. E2F1-3 are expressed at their peak levels during the G_1/S transition, indicating their crucial role in initiating DNA replication. E2F3b, E2F4, E2F5, E2F6, E2F7, and E2F8 constitute the repressor subclass of the E2F family. E2F4 and E2F5 are the critical E2F's at the G_0 checkpoint, serving to recruit pocket proteins, and other co-repressors to target promoters (Attwooll et al., 2004). The repression of their target genes is critical for holding the cell in a quiescent state. MEFs deficient for *E2f4* and *E2f5* do not repress G_0-specific targets and fail to proliferate in response to mitogenic signals (Gaubatz et al., 2000). E2F6, E2F7, and E2F8 are expressed at their peak levels during G_2/S, marking the end of DNA replication. They represent the only group of the E2F family lacking an Rb-binding domain, suggesting that they repress gene expression in a pocket protein-independent manner. E2F6 binds its targets as a member of a large, multi-subunit repressor that includes the polycomb proteins along with Mga and Max (Ogawa et al., 2002). The mechanism through which E2F7 and E2F8 bind to and repress target genes, on the other hand, is far less understood due to their recent discovery and lack of characterization.

E2F7 and E2F8 exhibit several structural characteristics that set them apart from the rest of the E2F family. As mentioned above, E2F7 and E2F8 lack the Rb-binding domain as well as the Marked Box (Mark.), which is involved in mediating interactions with cofactors (Figure 1). These two new E2Fs also lack the characteristic leucine-zipper domain that is required for dimerization with the partner proteins DP1/2. However, they possess two tandem DNA-binding domains (DBD) which allow them to bind DNA in a DP-independent manner (de Bruin et al., 2003; Di Stefano et al., 2003; Logan et al., 2004; Christensen et al., 2005; Logan et al., 2005; Maiti et al., 2005). These distinctive

structural features indicate that E2F7 and E2F8 function as a unique arm of the E2F family.

Previous work has shown that the individual deletion of *E2f7* or *E2f8* in mice results in no observable phenotypes. However, embryos lacking both *E2f7* and *E2f8* exhibit widespread apoptosis and die by embryonic day 11.5 (E11.5) (Li et al., 2008). The apoptosis was shown to be E2F1 and p53 dependent, as the concomitant loss of either *E2f1* or *p53* suppressed the ectopic apoptosis. However, these embryos still died by E11.5, indicating that fetal apoptosis was not the cause of death. The tissues, molecular pathways, and cellular processes disrupted in $E2f7^{-/-}/E2f8^{-/-}$ (Double knockout, DKO) embryos that led to their lethality remain completely unknown. In this study, we aim to directly address these questions and further characterize the function of E2F7 and E2F8. Utilizing a conditional knockout system, we demonstrate that the function of E2F7 and E2F8 in the placenta is both necessary and sufficient to carry the embryo to term. We also show that the critical action of E2F7/E2F8 involves regulating the G_1/S transition, involving a critical interaction with E2F3a. In conclusion, we demonstrate throughout this study that the repressive function of E2F7 and E2F8 is critical for the control of cell cycle progression.

Materials and Methods

Mouse Strains and Genotyping.

The conventional and conditional *E2f7, E2f8* knockout mice, *Sox2-cre, Cyp19-cre* transgenic mice, and Rosa26 reporter mice were maintained on a mixed 129SvEv; C57B/L6; FVB background. Three allele-specific primers were used for *E2f7* and *E2f8*

PCR genotyping: E2F7-a, 5'-AGGCAGCACACTTGACACG-3'; E2F7-b, 5'-ACTTTTGGGACAGAGGGTAGGA-3'; E2F7-c, 5'-CCAAGATGAAGGCCGAGATGCTAC-3'; or E2F8-a, 5-TAAAAAGCTTTGCGGTCGTT-3'; E2F8-b, 5'-AAGCCAACCTCGATCAATTG-3'; E2F8-c, 5-CTCGCATCATCGTCTGCT-3'

Quantitative RT-PCR (qRT-PCR)

Total RNA was extracted using Qiagen RNA miniprep columns according to the manufacturer's protocol, which included the optional DNase treatment before elution from the column. Reverse transcription of total RNA was performed using Superscript III reverse transcriptase (Invitrogen) and RNAse Inhibitor (Roche) as described by the manufacturer. Quantitative PCR was performed using *SYBR* Green reaction mix (BioRad) and the BioRad iCycler PCR machine. All reactions were performed in triplicate and relative amounts of cDNA were normalized to *Gapdh*. Primer sequences are available upon request.

***In situ* Hybridization**

In situ hybridization was performed on E9.5 (*Proliferin*) and E10.5 (*Tpbp*) placenta sections using a previously reported protocol (Christensen et al., 2002) that was modified for paraffin-embedded sections. These modifications were deparaffinization in xylene and Proteinase K (1 µg/ml) digestion. Plasmids for *Proliferin* and *Tpbp* (gifts from Dr. J. Rossant) were linearized with *HindIII* and *XbaI*, respectively, to generate templates for riboprobe synthesis. Radiolabeled probes were generated by *in vitro* transcription with

either T7 (*Proliferin*) or T3 (*Tpbp*) RNA polymerase (Roche) using both ^{35}S-CTP and ^{35}S-UTP. The probes were hydrolyzed at 60°C for 20 minutes in bicarbonate buffer (80 mM $NaHCO_3$, 120 mM Na_2CO_3). Hybridizations were performed with $1x10^7$ dpm/slide for each probe. Following application of the autoradiography emulsion NTB (Kodak), the slides were exposed for 1 day (*Proliferin*) or 3 days (*Tpbp*) before the emulsion was developed.

Histological Analysis and Immunostaining

Placenta samples were fixed in 10% neutral buffered formalin and embedded in paraffin. 5μm-thick sections were prepared. Standard hematoxylin and eosin (H&E) staining was used for general histopathological analysis. For immunostaining, slides were probed with primary antibodies specifically against E2F7 (ab56022, Abcam), E2F8 (homemade polyclonal antibody raised against a peptide representing amino acids 576-595 of murine E2F8), and Phospho-Histone 3 (P-H3, Ser10) (06-570, Millipore). Vectastain Elite ABC reagent (Vector labs) and DAB peroxidase substrate kit (Vector labs) were used in combination to immunohistochemically detect E2F7, E2F8, and P-H3 signals by following the manufacturer's instructions. Samples were counterstained with hematoxylin.

Cells under M phase of cell cycle and/or belonging to giant cell lineage were detected by immunofluorescence (IF) staining using P-H3 and PL-1 antibodies. Giant cells under G_1/S transition of endocycle were detected by double IF staining using BrdU (MO-0744, DAKO) and PL-1 (A gift from Dr. F Talamantes) antibodies. Nuclear DNA was counterstained with DAPI.

BrdU Assay

Pregnant females at 10.5 days postcoitum were injected intraperitoneally with BrdU (100 µg/grams of body weight) 30 min prior to harvesting. Samples were fixed in formalin and 5µm paraffin embedded-sections were used. After deparaffinization, anti-BrdU antibodies were used to detect BrdU incorporation according to the manufacturer's instructions. BrdU-stained slides were counterstained with DAPI and hematoxylin, respectively.

Affymetrix Microarray Analysis

Total RNA was isolated using Qiagen RNA miniprep columns according to the manufacturer's protocol. Global gene expression analyses were performed on Affymetrix Mouse Genome 430 2.0 arrays at the Ohio State University Comprehensive Cancer Center (www.osuccc.osu.edu/microarray/). Expression values were adjusted by quantile normalization and log2 transformation with RMAExpress and data was analyzed with BRB-ArrayTools 3.7.0 (http: linus.nci.nih.gov BRB-ArrayTools.html). Class comparison was used to select genes differentially expressed at a significance level of $p<0.05$. Probes with a >2-fold misexpression in $E2f7^{-/-};E2f8^{-/-}$ when compared to $E2f7^{+/+};E2f8^{+/+}$ were used and the average relative expression level of each genetic group was loaded into the TIGR MultiExperiment Viewer (MEV, version 4.0) (TIGR, Rockville, MD) to generate heatmaps. Clustering and scatter plot analyses were

performed by using Clustering and Scatterplot functions on BRB Array Tools. Promoter sequences of each gene (-1000bp ~ +300bp) were obtained from UCSC genome browser (http://genome.ucsc.edu/). TFSearch (http://www.cbrc.jp/research/db/TFSEARCH.html) aided in the identification of genes containing E2F consensus binding sites.

Chromatin Immunoprecipitation (ChIP)

For ChIP assays, the EZ CHIP^{TM} assay kit (Upstate Biotech) was used as described by the manufacturer. Briefly, HEK 293 cells overexpressing flag-E2F7, flag-E2F8 wild type or flag-E2F7DBD1-2, flag-E2F8DBD1-2 DNA binding mutant forms were crosslinked, lysed and sonicated followed by incubation with 2µg of anti-flag (M2, Sigma) or normal mouse IgG (Oncogene) antibodies at 4°C overnight. Antibody-protein-DNA complexes were recovered by addition of 30µl of Salmon Sperm DNA/Protein G agarose slurry (Upstate Biotech). Immunoprecipitated DNA fractions were decrosslinked and purified through Qiaquick columns (Qiagen). Real-time PCR quantification of ChIP samples was performed using the Biorad iCycler machine with primers specific for the indicated promoter regions. Reactions were performed in triplicate and normalized using the threshold cycle number for the total input sample. Sequences of primers are available upon request.

Confocal Microscopy and 3D Reconstruction

Placenta samples were collected from E10.5 mutant and control embryos, fixed with 4% paraformaldehyde overnight at 4°C and embedded in OCT. 70µm-thick frozen sections were cut, washed with 0.2% Triton-X in PBS for 1.5 hours and stained with 1mM Draq5

(Biostatus) at 4°C overnight. Draq5-stained samples were examined by confocal laser scanning microscopy (Zeiss LSM 510) with the use of a 63X objective and 0.7X scan zoom. Optical sections with between-plane-plane resolution of 0.40μm and axial resolution of 0.42μm were acquired. Four to five separate regions were imaged with a field of view of 207μm x 207μm and depth of 40 ± 2μm resulting in a stack of 100 images for each region. For 3D reconstruction, the image stacks were processed using Insight Toolkit and ITK-SNAP (Yushkevich et al., 2006). Each cell nucleus was segmented by active contour segmentation using region competition as the stopping criterion (Zhu and Yuille, 1996). Nuclei of binucleated and multinucleated cells were constructed separately and assigned different colors.

Transmission Electron Microscopy (TEM)

E10.5 placentas were harvested and fixed with 3% glutaraldehyde in 0.1M phosphate buffer overnight at 4°C. Following fixation, tissues were processed according to TEM Fixation Protocol (http://cmif.osu.edu/419.cfm) and embedded in Eponate resin for TEM observations. Ultrathin cross sections of placenta (70nm) were mounted on copper grids, double stained with uranyl acetate and lead citrate, and observed with a Technai G2 Spirit transmission electron microscope (FEI).

Quantification and Statistical Analysis

Images of immunostained sections were captured using Eclipse 50i (Nikon) and Axioskop 40 (Zeiss) microscopes and quantified using Metamorph Imaging 6.1 software.

Quantification of BrdU-postive cells was achieved by calculating the percentage of positive cells in the different regions or in the different cell lineages. Counting data are reported as the average ± SD fold induction of percentage of positive cells. Three sections per sample and at least three different samples for each genotype were analyzed. Results were represented as the average ± SD percentage of binucleated cells from three different samples. At least 143 giant cells were counted for each genotype group.

X-gal Staining

Whole-mount samples or 10μm frozen sections were fixed in 2% formaldehyde and 0.2% glutaraldehyde in PBS for 1.5 hours, and then washed 3 times for 5 minutes each in PBS at room temperature. Staining was carried out in 1mg/ml X-gal, 5mM potassium ferrocyanide, and 5mM potassium ferricyanide in lacZ wash buffer (0.01% deoxycholate, 0.02% NP-40 and 2mM $MgCl_2$) at 37°C overnight. Nuclear Fast Red counterstaining was used to visualize lacZ-negative cells from the frozen sections.

Results

Conventional knockout of *E2f7* and *E2f8* leads to profound placental defects

Previous work has shown that E2F7 and E2F8 are critical for mouse embryonic viability during mid-gestation, as their combined deletion results in embryonic lethality by day 11.5 (E11.5) (Li et al, 2008). This study is focused on further characterizing the dysfunction caused by the deletion of *E2f7/E2f8* that led to mid-gestation lethality. We reasoned that the identification of the tissues in which E2F7 and E2F8 play a critical role

in maintaining embryo viability would provide valuable insight into their physiological and molecular functions.

Embryos supplied with a non-functional placenta often show severe growth and developmental retardation, sometimes leading to lethality during mid-gestation (Rossant and Cross, 2001; Watson and Cross, 2005). Therefore, we deemed it prudent to further investigate placental defects exhibited in *E2f7*$^{-/-}$*/E2f8*$^{-/-}$ mice. Quantitative RT-PCR (qRT-PCR)showed relatively high expression of both *E2f7* and *E2f8* in the placenta as compared to the fetus, indicating that they play a more critical role in extra-embryonic cell lineages than in embryonic cell lineages (Figure 2a). Immunohistochemistry (IHC) staining confirmed that E2F7 and E2F8 are highly expressed at the protein level in each of the three main cell lineages of the placenta: Trophoblast Giant Cells (TG), Spongiotrophoblast (ST), and Labyrinth Trophoblast (LT) (Figure 2b). The expression of E2F7 and E2F8 appeared a bit odd however, as they were expressed highly in some cells and not at all in others, which served as a reflection of their cell cycle-dependent expression (de Bruin et al., 2003; Di Stefano et al., 2003; Maiti et al., 2005). We then examined Hematoxylin and Eosin (H&E)-stained sections of placenta to assess any gross physiological defects that may result in *E2f7*$^{-/-}$*/E2f8*$^{-/-}$ placentas (Figure 3a). In wild-type tissue at E10.5, H&E staining shows well organized tissue, with vasculature arranged as maternal sinusoids juxtaposed to fetal-derived blood vessels. The placental structure in *E2f7*$^{-/-}$*/E2f8*$^{-/-}$ embryos, however, was highly disorganized. These placentas exhibited abnormal clustering of trophoblast tissue that failed to invade the maternal decidua as well as a poorly developed vasculature network. Expression levels of cell lineage markers also highlighted the importance of E2F7 and E2F8 in tissue differentiation

(Figure 3b). While certain trophoblast stem cell markers (*Eomes* and *Cdx2*) were expressed at normal levels in *E2f7*$^{-/-}$*/E2f8*$^{-/-}$ tissue, the expression of SP and TG specific markers (*Tpbg*, *Pgfp*; and *Proliferin*, *Csf1r*, *Pl-1*, and *Prp*, respectively) was greatly reduced. *In situ* hybridization allowed us to visually confirm the decrease of *Tpbp* and *Proliferin* in the DKO placenta (Figure 3c and 3d). From these combined results, we were able to confirm that the placenta in *E2f7*$^{-/-}$*/E2f8*$^{-/-}$ embryos exhibits severe structural and cellular defects, suggesting that E2F7 and E2F8 play a critical role in the differentiation of this tissue during mid-gestation.

Extra-embryonic function of E2F7 and E2F8 is both necessary and sufficient for embryonic viability

Because of the high expression levels of E2F7 and E2F8 in extra-embryonic lineages as well as the severe defects observed in the placenta of *E2f7*$^{-/-}$*/E2f8*$^{-/-}$ embryos, we decided to more rigorously investigate the roles of E2F7 and E2F8 in the placenta. By utilizing the Cre-LoxP transgenic system, we were able to selectively disrupt *E2f7* and *E2f8* in a tissue-specific manner. To do this, we bred *E2f7*$^{LoxP/LoxP}$*/E2f8*$^{LoxP/LoxP}$*/Rosa26*$^{+/LoxP}$ mice to *Sox2*$^{+/cre}$ mice, generating mice that were *E2f7/E2f8* deficient in the embryonic compartment, but were supplied with a wild type placenta. *Sox2-cre* mice will express Cre-recombinase in the embryo proper, but not placenta, as early as E6.5 (Hayashi et al., 2002). The *Rosa26*$^{+/loxp}$ gene served as a reporter gene to allow for visual confirmation of Cre-recombinase expression via X-gal staining (Soriano, 1999). The efficiency and specificity of deletion was confirmed first by genotyping a variety of tissues via PCR, then visually by performing X-gal staining on E12.5 embryos and at birth (P0 pups)

(Figures 4c and 4d). Amazingly, these animals were discovered to be alive at all stages of embryonic development up until P0, although any pups that did survive through birth were severely runted and died shortly thereafter (Figure 4a). At E10.5, the embryos showed none of the obvious phenotypes associated with *E2f7*$^{-/-}$*/E2f8*$^{-/-}$ embryos, indicating that the embryo proper is not the critical tissue for E2F7/E2F8 function during mid-gestation (Figure 4b). This also gave us some perspective as to just how important the placenta was for E2F7/E2F8 function, as it is able to carry the pregnancy to term.

To reconfirm that the placenta is the critical compartment for E2F7/E2F8 function, we again used the Cre-LoxP transgenic system. This time we aimed to disrupt endogenous *E2f7/E2f8* in the placenta by breeding our *E2f7*$^{loxp/loxp}$*/E2f8*$^{loxp/loxp}$*/Rosa26*$^{+/loxp}$ mice to *Cyp19*$^{+/loxp}$ mice, resulting in the specific deletion of *E2f7/E2f8* in extra-embryonic cell lineages. *Cyp19-cre* mice express Cre-recombinase by E6.5 in all trophoblast cell lineages, but not in the embryonic compartment (Wenzel and Leone, 2007). The specificity and efficiency of these deletions were again confirmed via PCR genotyping of placenta and fetus, as well as X-gal staining (Figures 5c and 5d). The results highlight the importance of E2F7 and E2F8 function in the placenta, as their conditional deletion in the placenta completely recapitulated the phenotypes observed in the conventional double knockout embryos. By E10.5, approximately half of the embryos had died, and all were dead by E11.5 (Figure 5a). These embryos were developmentally retarded (visibly smaller than wild type) by E9.5 (Figure 5b). Associated with this growth retardation was the disruption of placental architecture as seen in *E2f7*$^{-/-}$*/E2f8*$^{-/-}$ mice, as well the dilation of blood vessels in and

around the umbilical cord (Figure 5b). These genetic analyses provide evidcene that the placenta is the critical compartment for E2F7 and E2F8 function during mid-gestation.

Loss of E2F7 and E2F8 in the placenta dictates molecular events in the fetus

As both E2F7 and E2F8 act as transcription factors, we assumed that the misregulation of its gene targets was likely the underlying reason for many of the severe phenotypes observed. To explore this hypothesis, we used Affymetrix microarrays to compare global gene expression in fetal tissue derived from *E2f7*$^{+/+}$*/E2f8*$^{+/+}$ and *E2f7*$^{-/-}$*/E2f8*$^{-/-}$ mice. In order to discriminate between direct and placenta-induced indirect changes in gene expression we also included *Sox2*$^{+/cre}$*/E2f7*$^{-/loxp}$*/E2f8*$^{-/loxp}$ (*Sox2-cre*), and *Cyp19*$^{+/cre}$*/E2f7*$^{-/loxp}$*/E2f8*$^{-/loxp}$ (*Cyp19-cre*) embryos as well. All embryos were harvested at day E10.5. We began by comparing overall expression patterns across the four groups, and ended with gene-specific annotation of E2F7/E2F8 direct targets.

Unsupervised clustering of the entire set of fetal expression data segregated the four genotypic sets into two arms. *E2f7*$^{+/+}$*/E2f8*$^{+/+}$ and *Sox2-cre* fetuses segregated to one arm and *E2f7*$^{-/-}$*/E2f8*$^{-/-}$ and *Cyp19-cre* fetuses segregated to the other (Figure 6). This was remarkable in that fetuses with opposite genotypes segregated together. In one arm, *Sox2-cre* did segregate from *E2f7*$^{+/+}$*/E2f8*$^{+/+}$, indicating that the disruption of *E2f7* and *E2f8* in the fetus does result in some cell autonomous gene misexpression. In the other branch however, *E2f7*$^{-/-}$*/E2f8*$^{-/-}$ and *Cyp19-cre* fail to segregate from one another, despite the fact that *Cyp19-cre* fetuses expressed functional E2F7 and E2F8 and *E2f7*$^{-/-}$*/E2f8*$^{-/-}$ fetuses did not. These results highlight the importance of placental E2F7 and E2F8 in not only determining the health and viability of the fetus, but also their molecular readouts.

Identification of Direct Targets of E2F7 and E2F8

We then performed global expression analyses on *E2f7*$^{+/+}$*/E2f8*$^{+/+}$, *E2f7*$^{-/-}$*/E2f8*$^{-/-}$, *Sox2-cre* and *Cyp19-cre* E10.5 placentas. Unsupervised clustering analysis separated the four genetic groups into two arms again, with *E2f7*$^{+/+}$*/E2f8*$^{+/+}$ and *Sox2-cre* cohorts clustering together in one arm and *E2f7*$^{-/-}$*/E2f8*$^{-/-}$ and *Cyp19-cre* cohorts clustering in the other arm (Figure 7a). As in the analysis for the fetuses, the clustering pattern was based on the genotype of the placenta, again highlighting the critical role of placental E2F7 and E2F8 in determining molecular events. However, we did observe differences in clustering between *E2f7*$^{+/+}$*/E2f8*$^{+/+}$ and *Sox2-cre* placentas and between *E2f7*$^{-/-}$*/E2f8*$^{-/-}$ and *Cyp19-cre* placentas, indicating that fetal E2F7/E2F8 do have an effect on placental gene expression.

E2F7 and E2F8 are believed to act as transcriptional repressors. In order to identify direct targets repressed by E2F7/E2F8, we focused on genes that were upregulated in tissues lacking *E2f7/E2f8*. We analyzed both *E2f7*$^{-/-}$*/E2f8*$^{-/-}$ and *Cyp19-cre* placentas and found a subset of 49 genes that were upregulated >2 fold in both genotypic classes (Figure 7b). We then confirmed these results via qRT-PCR on a subset of the 49 genes (data not shown). Characterization of these genes indicated an enrichment of genes with functions related to metabolism, placental development, and cell cycle regulation (Figure 7c).

We then proceeded to determine which, if any, of these 49 genes were also upregulated in fetuses lacking *E2f7/E2f8*. While we considered the use of both *E2f7*$^{-/-}$*/E2f8*$^{-/-}$ and *Sox2-cre* microarrays for this analysis, we decided to only analyze the *Sox2-*

cre array in an effort to avoid non-autonomous gene misregulation in the fetus caused by placental defects. We included all genes whose expression was induced >1.5 fold in our analysis. We found that 20 of the 49 genes were regulated in a non-tissue specific manner, as their expression levels increased in any tissue lacking *E2f7/E2f8* (Figure 8a). We classified the other 29 genes as placenta-specific targets, considering they were not upregulated in the fetus. Promoter analysis on TFSearch indicated that 85% of the 20 gene subset (17/20) featured conserved E2F binding sites on their promoters, suggesting an enrichment of E2F target genes in this set. On the other hand, only ~10% of the placenta-specific genes contained E2F binding sites on their promoters, indicating that they are likely regulated indirectly or through atypical binding sites.

We then performed a series of chromatin immunoprecipitations (ChIP) to determine which genes from the 20 gene set were truly direct targets of E2F7 and E2F8. Because reliable mouse E2F7/E2F8-specific ChIP-grade antibodies are not available, we overexpressed flag-tagged E2F7/E2F8 in human embryonic kidney cells (HEK 293) and performed ChIP assays with flag-specific antibodies. We tested nine different promoters, focusing on regions that contained consensus E2F binding sites, and found that anti-flag antibody efficiently co-immunoprecipitated all nine promoter sequences (Figure 8b). Control IgG antibodies did not immunoprecipitate target sequences, and flag antibodies did not immunoprecipitate irrelevant sequences in *E2f1* (exon 1) or on the *tubulin* promoter. From these results, we conclude that these 20 genes are *bona fide* targets of E2F7 and E2F8 *in vivo*. Interestingly, these 20 targets encode genes involved in cell cycle regulation (Figure 9). The 29 placenta-specific genes encoded proteins involved metabolism and placenta development (Figure 10).

Loss of *E2f7/E2f8* results in ectopic DNA replication

The high percentage of cell cycle related direct targets prompted us to examine the *E2f7*$^{-/-}$*/E2f8*$^{-/-}$ placentas for cell cycle defects. To this end, we measured DNA synthesis via BrdU incorporation in each of the three major extra-embryonic cell lineages. Our analysis revealed ectopic replication in both the TG and ST lineages, but not in the LT lineage (Figures 11a and 11b). We then asked whether this ectopic DNA replication is also present in the embryonic compartment. However, fetal tissue during mid-gestation undergoes such high endogenous levels DNA replication that ectopic replication cannot be detected. Therefore, we decided to obtain more differentiated tissue from the lung of *Sox2-cre* pups at P0. We again noticed ectopic DNA replication in *Sox2-cre* pups (Figures 11c and 11d). These findings together strongly suggest that E2F7 and E2F8 play a novel role in regulating the G_1/S checkpoint in a tissue non-specific manner.

Loss of E2F3a Rescued Placental Defects and Lethality of *E2f7* and *E2f8* Double Mutant Embryos

Knowing that E2F7 and E2F8 play a critical role in regulating the G_1/S checkpoint, we wanted to further characterize its function in regulating cell progression into S phase. Our analysis of the G_1/S-specific targets then led us to consider E2F3a, which is known to regulate many of the same targets. E2F3a serves as a potent transcription activator, and functions in stimulating the cell through G_1 and into S phase (Danielian et al., 2008; Chong et al., 2009). We hypothesized then that the loss E2F7 and E2F8 would lead to an increase in E2F3a activity at the G_1/S checkpoint, resulting in ectopic DNA replication.

If E2F3a was indeed overactive in the absence of E2F7/E2F8, then the additional deletion of *E2f3a* in double knockout mice might rescue the ectopic DNA replication. We therefore proceeded to breed *E2f7*$^{+/-}$*/E2f8*$^{-/-}$ mice to *E2f3a*$^{-/-}$ mice to obtain *E2f3a*$^{+/-}$*/E2f7*$^{+/-}$*/E2f8*$^{+/-}$ offspring. We then crossed these offspring to obtain *E2f3a*$^{-/-}$*/E2f7*$^{-/-}$*/E2f8*$^{-/-}$ (Triple Knockout; TKO) embryos. Amazingly, all TKO offspring were viable at E11.5, and some even survived to term, dying shortly after birth (Figure 12a). Analysis of H&E staining of the E10.5 placenta showed that the additional deletion of *E2f3a* fully restored the structure and vascular network of the placenta (Figure 12b). From these results, we are convinced that the increase in E2F3a function is the leading cause of placental dysfunction and mid-gestation lethality.

To address the well known role of E2F3a in stimulating DNA replication, we then asked whether the ablation of *E2f3a* would rescue the ectopic DNA synthesis observed in *E2f7*$^{-/-}$*/E2f8*$^{-/-}$ placentas. We measured DNA synthesis in both the ST and TG lineages of the placenta. The analysis revealed a full rescue of the ectopic DNA synthesis in the *E2f3a*$^{-/-}$*/E2f7*$^{-/-}$*/E2f8*$^{-/-}$ placentas (Figure 11c). These results taken together indicate that an increase in E2F3a activity is the cause of ectopic DNA synthesis observed in *E2f7*$^{-/-}$*/E2f8*$^{-/-}$ placentas, and that this aberrant DNA synthesis is the major contributor to placental dysfunction. We conclude then that E2F7 and E2F8 play a critical role in regulating the progression from G_1 to S phase, and that the ectopic S phase entry in *E2f7*$^{-/-}$*/E2f8*$^{-/-}$ placentas is the leading contributor to mid-gestation lethality.

Loss of *E2f7/E2f8* Results in Aberrant Mitosis in Trophoblast Giant Cells

Although the ectopic DNA replication is the leading contributor to embryonic we had already analyzed the role E2F7/E2F8 at the G_1/S transition, we next asked whether it also played a role at the G_2/M checkpoint. To this end, I determined the percentage of cells undergoing mitosis via IHC staining with antibodies specific for phosho-Histone 3 (p-H3) (Figure 13a). Our analysis revealed a significant induction in TG cells, but not in ST or LT lineages (Figure 13b). This result was particularly surprising in that TG cells do not perform a typical cell cycle, but instead undergo repeated rounds of DNA replication with no mitosis, known as the endocycle. Because the departure from an endocycle into a typical cell cycle is such a unique phenotype, we sought to visualize this phenomenon. For this purpose, we performed a Draq-5 stain then utilized Confocal microscopy, giving us 3D renderings of the nuclei (Figure 13c). Surprisingly, these images indicated that the *E2f7/E2f8* deficient Trophoblast Giant cells were not undergoing normal mitoses. Instead, they underwent karyokinesis without cytokinesis, producing multi-nucleated cells, which we confirmed using electron microscopy (Figure 13d). A significant induction in multinucleated giant cells was observed in $E2f7^{-/-}/E2f8^{-/-}$ placentas (Figure 13e). Though the mechanism behind this unusual mitosis remains unclear, we hypothesize that the APC/C required for cytokinesis is regulated through a different pathway, and is therefore is not susceptible to *E2f7/E2f8* deficiency.

We then asked whether the ectopic karyokinesis would be rescued by the additional ablation of *E2f3a*. Analysis of p-H3 staining showed that there was no rescue of the mitotic phenotype, and multinucleated giant cells were still present in the placenta (Data not shown). This result indicates that although E2F7 and E2F8 are critical in

regulating both the G_1/S and G_2/M transitions, these transitions are not connected, as the rescue of ectopic DNA replication does not result in the rescue of ectopic M phase entry. This also serves to confirm our conclusion that aberrant S phase entry is the leading contributor to placental dysfunction and embryonic lethality.

E2F7/E2F8 Work in Concert with Rb and Related Pocket Proteins

While investigating the functional role of E2F7/E2F8 in regulating cell cycle progression, we were also examining the genetic link between E2F7/E2F8 and pRb/p107/p130 (pocket protein family). It is well documented that the interactions between the E2f family and pocket protein family are critical for the proper cell cycle progression. However, the mechanism through which the pocket proteins bind DNA remains unknown. Because *Rb*$^{-/-}$ embryos bear a high resemblance to *E2f7*$^{-/-}$*/E2f8*$^{-/-}$, we hypothesized that E2F7 and E2F8 could act as the critical downstream binding partners for pRb. *Rb*$^{-/-}$ mice show severe placental defects, resulting in embryonic lethality (Wu et al, 2003). Also, pRb function in the placenta is both necessary and sufficient to carry an embryo to term (Wenzel et al, 2007). The only major difference observed between *Rb*$^{-/-}$ and *E2f7*$^{-/-}$*/E2f8*$^{-/-}$ embryos is the exact time point of lethality, with *E2f7*$^{-/-}$*/E2f8*$^{-/-}$ embryos dying by E11.5 and *Rb*$^{-/-}$ embryos dying between E13.5 and E16.5.

I then aimed to determine the reason for the discrepancy between the lethality time points. We hypothesized that the *Rb*$^{-/-}$ mice survived longer due to compensation from the other pocket proteins, p107 and p130. We therefore crossed *Rb*$^{+/-}$*/p107*$^{+/-}$ with *Rb*$^{+/-}$*/p107*$^{+/-}$ and *Rb*$^{+/-}$*/p130*$^{+/-}$ with *Rb*$^{+/-}$*/p130*$^{+/-}$ to obtain *Rb*$^{-/-}$*/p107*$^{-/-}$ and *Rb*$^{-/-}$*/p130*$^{-/-}$ embryos, respectively. Genotyping analysis revealed that the additional ablation of *p130*

had no effect on the time of embryonic lethality, but preliminary data indicates that *Rb*$^{-/-}$*/p107*$^{-/-}$ embryos die at a similar time point as *E2f7*$^{-/-}$*/E2f8*$^{-/-}$ embryos (Figure 14a and 14b). We therefore hypothesize that p107 is the other pocket protein that interacts with E2F7/E2F8.

Continuing our investigation into the nature of the genetic interaction between E2F7/E2F8 and Rb/p107, we decided to set up breedings between the two genetic groups in order to obtain pups that were heterozygous for each of the four genes. I hypothesized that if these four proteins function cooperatively, then the loss of one allele per gene may produce an observable phenotype. However, these mice were viable both at birth (P0) and 21 days post birth (P21) at the predicted Mendelian ratios. We then bred mice to obtain *E2f7*$^{+/-}$*/E2f8*$^{-/-}$*Rb*$^{+/-}$*/p107*$^{+/-}$ or *E2f7*$^{-/-}$*/E2f8*$^{+/-}$*Rb*$^{+/-}$*/p107*$^{+/-}$ pups, containing one fewer allele than the previously described quadruple heterozygous mice. Our early results indicate that losing an additional allele of either *E2f7* or *E2f8* results in decreased viability, as these mice survive to P21 at a lower rate than Mendelian ratios would predict (Figure 15). We then analyzed viability at P0, and found viable *E2f7*$^{-/-}$*/E2f8*$^{+/-}$*Rb*$^{+/-}$*/p107*$^{+/-}$ pups at nearly Mendelian ratios, whereas *E2f7*$^{+/-}$*/E2f8*$^{-/-}$*Rb*$^{+/-}$*/p107*$^{+/-}$ pups were viable at below expected numbers. If these results prove significant, they would serve to bolster the claim that E2F7 and E2F8 work in concert with pRb and p107.

Discussion

Conclusion

E2F7 and E2F8 constitute the most recently discovered, and therefore the least understood branch of the E2F family. In this study, we show that E2F7/E2F8 play a

critical role in maintaining the integrity of the extra-embryonic compartment during mid-gestation. This significance was demonstrated by a conditional knockout study that showed their activity in the placenta is both necessary and sufficient to carry embryos to term. Our analysis of global gene expression arrays in placental and fetal tissues then illuminated a unique transcriptional network regulated by E2F7 and E2F8. This transcriptional network proved critical in regulating the transition through the G_1/S checkpoint and suppressing mitotic entry in the endocycle. While disruption of this network was tolerated by *E2f7*$^{-/-}$/*E2f8*$^{-/-}$ embryos, it had catastrophic consequences in the spongiotrophoblast and trophoblast giant cells of the placenta, resulting in ectopic DNA replication and aberrant karyokinesis in giant cells. Together, these data provide convincing evidence for E2F7/E2F8-mediated control of mammalian cell cycle progression.

Future Direction

This study has made a significant contribution in defining the molecular role of E2F7 and E2F8 in embryonic development, but work still remains in illuminating their biological functions and molecular interactions. Our priority right now is to further define the physical interaction between E2F7/E2F8 and E2F3a at the G_1/S checkpoint. While we conclude that this interaction is critical for proper S phase entry, the nature of the interaction remains unclear. We are currently investigating the possibility of a competitive interaction at target promoters by performing a series of ChIP experiments in MEFs, to determine if E2F3a binds its target promoters at a higher rate in the absence of E2F7/E2F8. This analysis could reveal a novel interaction within the E2f family, as

members of the family have never before been observed to undergo competitive interactions as a mechanism of regulating cell cycle.

The newly discovered connection with E2F3a will likely carry important medical implications for E2F7 and E2F8 as well. E2F3a is noted to be upregulated in several forms of cancer, including prostate and bladder (Paulson et al., 2006). This is the result of an increase rate of cellular proliferation and an override of proper checkpoints transitions. This link, along with the already well established connection between the E2F family and cell cycle control, indicates a strong likelihood that E2F7 and E2F8 will be points of interest in future cancer studies.

Acknowledgements

I would like to thank Jing Li for her continued guidance, mentorship, and patience throughout the duration of this project. Dr. Gustavo Leone provided considerable amounts of guidance and financial support, without which this project would not have been possible. I would also like to thank John Thompson and Braxton Forde for their execution of certain protocols. Finally, I would like to thank the entire Leone lab for their continued support and guidance throughout this rather involved project.

References

Attwooll, C., Lazzerini Denchi, E., and Helin, K. (2004). The E2F family: specific functions and overlapping interests. EMBO J. *23*, 4709-4716.

Jean-Leon Chong, Shih-Yin Tsai, Nidhi Sharma, Rene Opavsky, Richard Price, Lizhao Wu, Soledad A. Fernandez, and Gustavo Leone (2009). *E2f3a* and *E2f3b* Contribute to the Control of Cell Proliferation and Mouse Development. Molecular and Cellular Biology, *29*, 414-424

Christensen, J., Cloos, P., Toftegaard, U., Klinkenberg, D., Bracken, A.P., Trinh, E., Heeran, M., Di Stefano, L., and Helin, K. (2005). Characterization of E2F8, a novel E2F-like cell-cycle regulated repressor of E2F-activated transcription. Nucleic Acids Res. *33*, 5458-5470.

Cam H, Dynlacht. 2003. Emerging roles for E2F: beyond the G1/S transition and DNA replication. *Cancer Cell* 3: 311-316.

Danielian, P. S., L. B. Friesenhahn, A. M. Faust, J. C. West, A. M. Caron, R. T. Bronson, and J. A. Lees. 2008. E2f3a and E2f3b make overlapping but different contributions to total E2f3 activity. *Oncogene 27***:**6561-6570.

de Bruin, A., Maiti, B., Jakoi, L., Timmers, C., Buerki, R., and Leone, G. (2003). Identification and characterization of E2F7, a novel mammalian E2F family member capable of blocking cellular proliferation. J Biol Chem. *278*, 42041-42049.

Di Stefano, L., Jensen, M.R., and Helin, K. (2003). E2F7, a novel E2F featuring DP-independent repression of a subset of E2F-regulated genes. EMBO J. *22*, 6289-6298.

Frolov, M.V., and Dyson, N.J. (2004). Molecular mechanisms of E2F-dependent activation and pRB-mediated repression. J Cell Sci. *117*, 2173-2181.

Gaubatz, S., Lindeman, G.J., Ishida, S., Jakoi, L., Nevins, J.R., Livingston, D.M., and Rempel, R.E. (2000). E2F4 and E2F5 play an essential role in pocket protein-mediated G1 control. Mol Cell. *6*, 729-735.

Hayashi, S., Lewis, P., Pevny, L., and McMahon, A.P. (2002). Efficient gene modulation in mouse epiblast using a Sox2Cre transgenic mouse strain. Mech Dev. *119*, S97-S101.

Li, J., Ran, C., Li, E., Gordon, F., Comstock, G., Siddiqui, H., Cleghorn, W., Chen, H.Z., Kornacker, K., Liu, C.G., et al. (2008). Synergistic function of E2F7 and E2F8 is essential for cell survival and embryonic development. Dev Cell. *14*, 62-75.

Logan, N., Delavaine, L., Graham, A., Reilly, C., Wilson, J., Brummelkamp, T.R., Hijmans, E.M., Bernards, R., and La Thangue, N.B. (2004). E2F-7: a distinctive E2F family member with an unusual organization of DNA-binding domains. Oncogene. *23*, 5138-5150.

Logan, N., Graham, A., Zhao, X., Fisher, R., Maiti, B., Leone, G., and La Thangue, N.B. (2005). E2F-8: an E2F family member with a similar organization of DNA-binding domains to E2F-7. Oncogene *24*, 5000-5004.

Maiti, B., Li, J., de Bruin, A., Gordon, F., Timmers, C., Opavsky, R., Patil, K., Tuttle, J., Cleghorn, W., and Leone, G. (2005). Cloning and characterization of mouse E2F8, a novel mammalian E2F family member capable of blocking cellular proliferation. J. Biol. Chem. *280*, 18211-18220.

Murray, A.W. (2004). Recycling the cell cycle: cyclins revisited. Cell *116*, 221-234.

Ogawa, H., Ishiguro, K., Gaubatz, S., Livingston, D.M., and Nakatani, Y. (2002). A complex with chromatin modifiers that occupies E2F- and Myc-responsive genes in G0 cells. Science *296*, 1132-1136.

Rossant, J., and Cross, J.C. (2001). Placental development: lessons from mouse mutants. Nat Rev Genet. *2*, 538-548.

Sánchez, I., and Dynlacht, B.D. (2005). New insights into cyclins, CDKs, and cell cycle control. Semin Cell Dev Biol. *16*, 311-321.

Soriano, P. (1999). Generalized lacZ expression with the ROSA26 Cre reporter strain. Nat. Genet. *21*, 70–71.

Watson, E.D., and Cross, J.C. (2005). Development of structures and transport functions in the mouse placenta. Physiology (Bethesda) *20*, 180-93.

Wenzel, P.L., and Leone, G. (2007). Expression of Cre recombinase in early diploid trophoblast cells of the mouse placenta. Genesis 45, 129-134.

Wenzel PL, Wu L, de Bruin A, Chong JL, Chen WY, Dureska G, Sites E, Pan T, Sharma A, Huang K, Ridgway R, Mosaliganti K, Sharp R, Machiraju R, Saltz J, Yamamoto H, Cross JC, Robinson ML, Leone G. (2007). Rb is critical in a mammalian tissue stem cell population. Genes Dev., 21, 85-97.

Lizhao Wu, Alain de Bruin, Harold I. Saavedra, Maja Starovic, Anthony Trimboli, Ying Yang, Jana Opavska, Pamela Wilson, John C. Thompson, Michael C. Ostrowski, Thomas J. Rosol, Laura A. Woollett, Michael Weinstein, James C. Cross, Michael L. Robinson, Gustavo Leone. Extra-embryonic function of Rb is essential for embryonic development and viability. Nature. 421. 942-947.

Figure 1

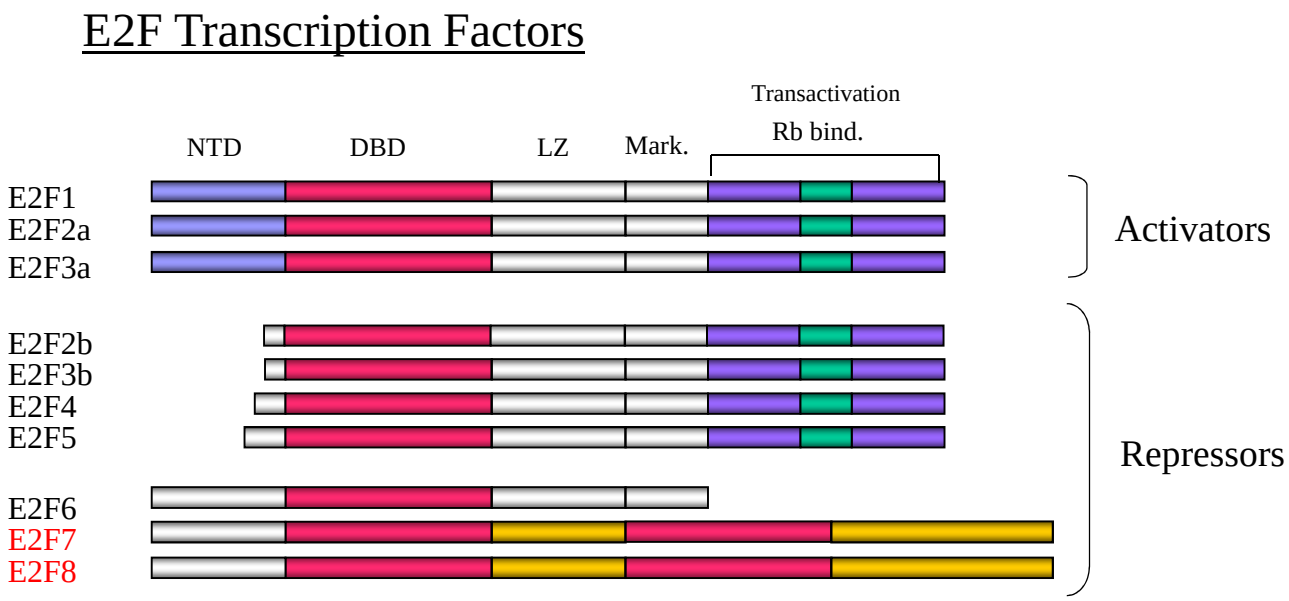

E2F family of transcription factors.

Schematic representations of E2F transcription factors. Eight distinct E2F gene loci encode for ten different E2F isoforms. A conserved DNA binding domain (DBD) is the feature that distinguishes each isoform as a member of the E2F family of transcription factors. The N-terminal domain (NTD) of E2F1-3 harbors the cyclin A-binding and Skp-binding domains and is distinct from the NTD of E2F6-8. The leuzine zipper (LZ) domain common to E2F1-6 is involved in dimerizing with DP1 or DP2, but is absent in E2F7-8. The Marked (Mark.) domain common to E2F1-6 is involved in mediating interactions with co-factors; The classical Rb binding (Rb bind.) domain buried within the activation domain is common to E2F1-5.

Figure 2

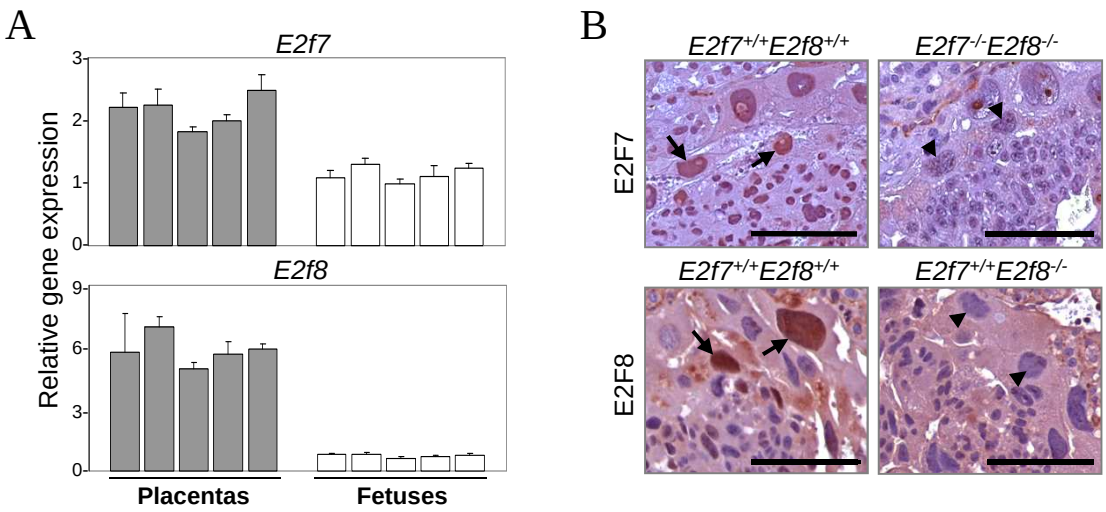

E2F7 and E2F8 express highly in the placenta (A) Real-time RT-PCR analysis of *E2f7* or *E2f8* expression in E10.5 wild type placentas (gray bars) and fetuses (white bars). (B) Immunohistochemistry using antibodies specific against E2F7 (top panels) and E2F8 (bottom panels) on E10.5 placenta sections with the indicated genotypes. Positive trophoblast giant cells are indicated by arrows.

Figure 3

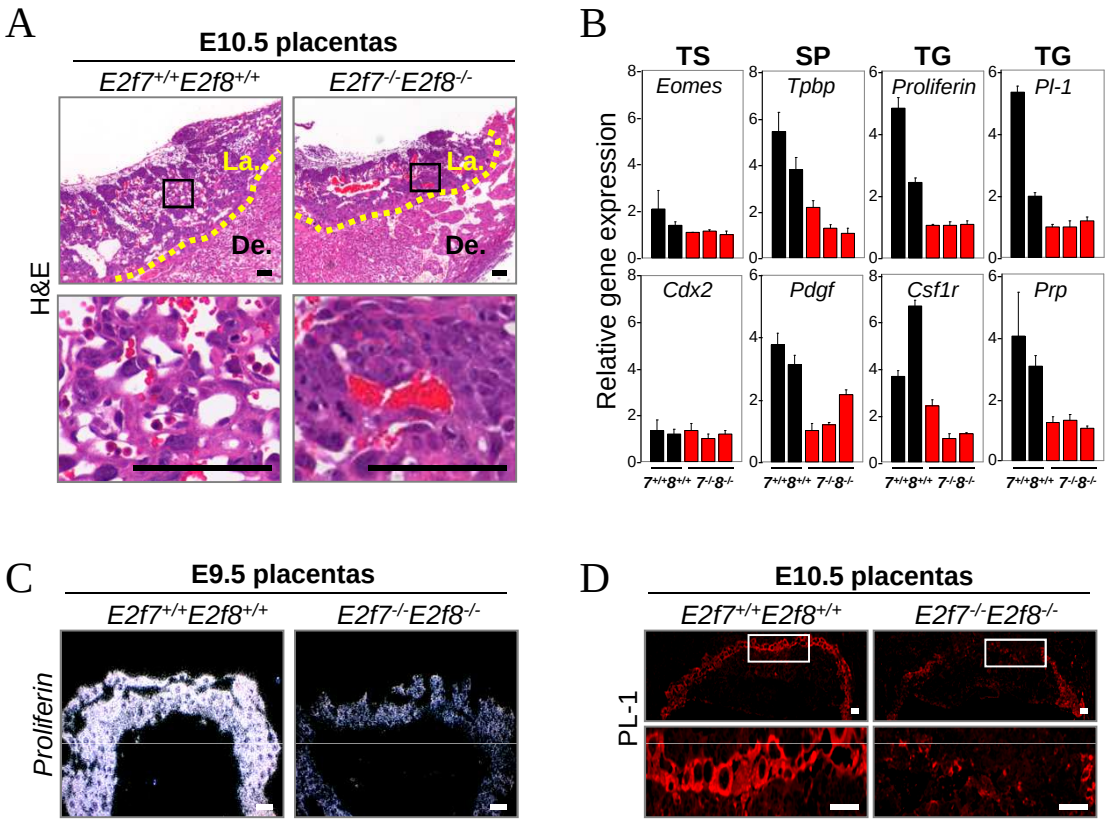

Profound Placental Defects in *E2f7*$^{-/-}$*E2f8*$^{-/-}$ Embryos. (A) E10.5 placenta sections with the indicated genotypes were stained with Hematoxylin and Eosin (H&E). The bottom panels are high magnification images of representative areas demarcated by the boxes in the top panels. De., Decidua; La., Labyrinth. (B) Real-time RT-PCR analysis of trophoblast cell lineage markers in E10.5 *E2f7*$^{+/+}$*E2f8*$^{+/+}$ ($7^{+/+}8^{+/+}$, black) and *E2f7*$^{-/-}$*E2f8*$^{-/-}$ ($7^{-/-}8^{-/-}$, red) placentas. TS, trophoblast stem cells; SP, spongiotrophoblast cells; TG, trophoblast giant cells. (C) RNA *in situ* hybridization analysis of *Proliferin*, a giant cell-specific marker, on E9.5 placenta sections having the indicated genotypes. (D) Immunofluorescence staining of E10.5 placenta sections with the indicated genotypes, using antibodies specific for Placental Lactogen 1 (PL-1), a giant cell-specific marker. The boxed areas in top panels are shown at higher magnification in bottom panels. All of the real-time RT-PCR data represent the average of samples analyzed in triplicate; error bars indicate average ± SD from triplicates. Scale bars, 100 µm.

Figure 4

A

Genotypic analysis of embryos: *Sox2-cre*

	$7^{loxp/+}$		$7^{loxp/-}$		*cre*;$7^{loxp/+}$		*cre*;$7^{loxp/-}$		total
	$8^{loxp/+}$	$8^{loxp/-}$	$8^{loxp/+}$	$8^{loxp/-}$	$8^{loxp/+}$	$8^{loxp/-}$	$8^{loxp/+}$	$8^{loxp/-}$	
E10.5	--	4	--	4	--	6	--	4[a]	28
expected	--	4	--	4	--	4	--	4	
E13.5	--	4	--	2	--	7	--	8[a]	21
expected	--	5	--	5	--	5	--	5	
P0-P1	5	19	4	18	3	19	6	11(8)[b]	93
expected	4	20	4	20	4	20	4	19	

() number of dead embryos; Fisher's exact test: [a] not significant (p<1.0); [b] highly significant (p<0.003) in comparison to the $7^{loxp/-}8^{loxp/-}$ embryos.

B

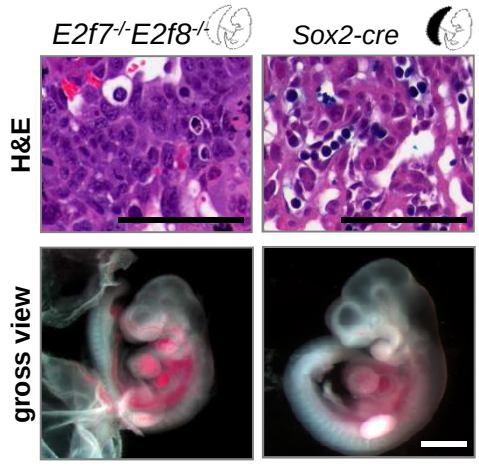

C

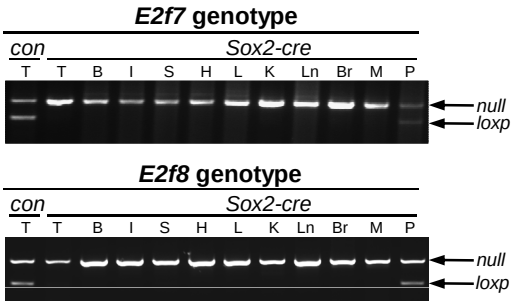

D

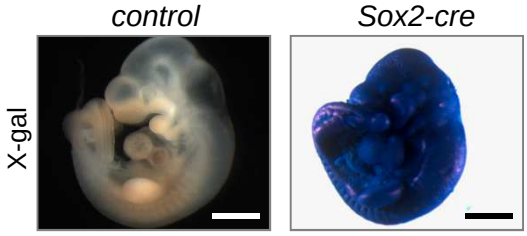

***E2f7* and *E2f8* in placenta are sufficient to sustain embryonic viability** (A) Genotypic analysis of embryos derived from *Sox2-cre* crosses at the indicated stages of development. *cre*, *Sox2-cre*; $7^{loxp/+}$, $E2f7^{loxp/+}$; $7^{loxp/-}$, $E2f7^{loxp/-}$; $8^{loxp/+}$, $E2f8^{loxp/+}$; $8^{loxp/-}$, $E2f8^{loxp/-}$. (B) Top panels: H&E staining of E10.5 placentas with the indicated genotypes. Scale bars, 100 µm. Bottom panels: Gross appearance of E10.5 fetuses having the indicated genotypes. Dilated blood vessels and hemorrhages are indicated by arrows. Note that the $E2f7^{-/-}$;$E2f8^{-/-}$ fetus is smaller in size. Scale bars, 1 mm. (C) Representative *E2f7* (top) and *E2f8* (bottom) PCR genotyping results using genomic DNA isolated from different organs of P0 pups. T, tail; B, bladder; I, intestine; S, stomach; H, heart; L, liver; K, kidney; Ln, lung; Br, brain; M, muscle; P, placenta. (D) Whole E10.5 $E2f7^{loxp/-}$;$E2f8^{loxp/-}$ (*control*) and *Sox2-cre*;$E2f7^{loxp/-}$;$E2f8^{loxp/-}$ (*Sox2-cre*) fetuses were stained X-gal. Scale bars, 1 mm. Embryo cartoons at the top of the panels represent fetuses and placentas with wild type (black) or double mutant (white) genotypes.

Figure 5

A

Genotypic analysis of embryos: *Cyp19-cre*

	$7^{loxp/+}$		$7^{loxp/loxp}$		*cre*;$7^{loxp/+}$		*cre*;$7^{loxp/loxp}$		total
	$8^{loxp/+}$	$8^{loxp/loxp}$	$8^{loxp/+}$	$8^{loxp/loxp}$	$8^{loxp/+}$	$8^{loxp/loxp}$	$8^{loxp/+}$	$8^{loxp/loxp}$	
E10.5	4	2	7(1)	21	3	9	10	14(8)[a]	79
expected	5	7	10	18	5	7	10	18	
E11.5	--	--	4	10	--	--	2	0(11)[a]	27
expected	--	--	3	11	--	--	3	11	

() number of dead embryos; Fisher's exact test: [a] highly significant (p<0.004) in comparison to the $7^{loxp/loxp}8^{loxp/loxp}$ embryos.

B

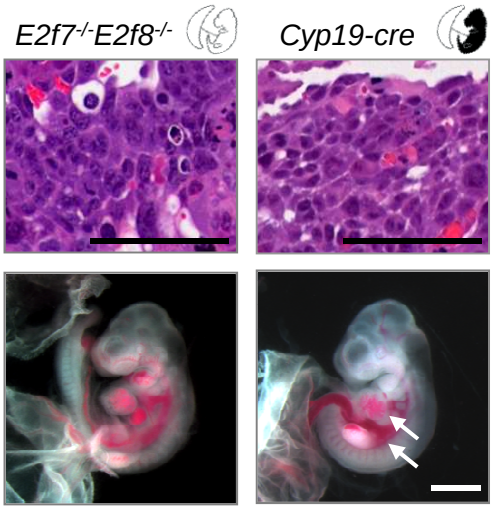

C

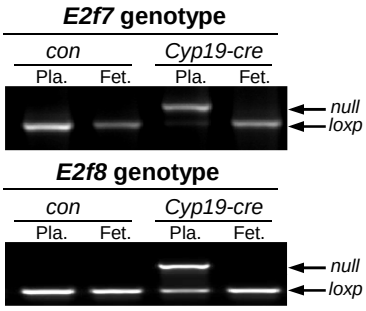

D

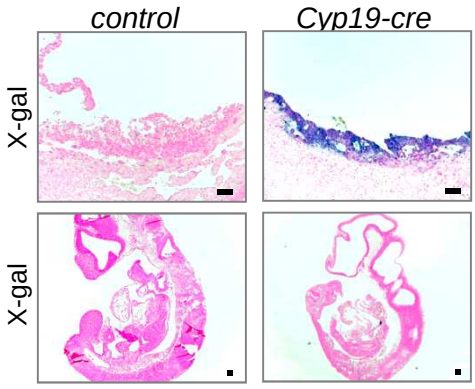

***E2f7* and *E2f8* in the placenta are required to sustain fetal viability** (A) Genotypic analysis of embryos derived from *Cyp19-cre* crosses at the indicated stages of development. *cre*, *cyp19-cre*; $7^{loxp/+}$, $E2f7^{loxp/+}$; $7^{loxp/loxp}$, $E2f7^{loxploxp}$; $8^{loxp/+}$, $E2f8^{loxp/+}$; $8^{loxp/loxp}$, $E2f8^{loxp/loxp}$. (B) Top panels: H&E staining of E10.5 placentas with the indicated genotypes. Scale bars, 100 µm. Bottom panels: Gross appearance of E10.5 fetuses having the indicated genotypes. Dilated blood vessels and hemorrhages are indicated by arrows. Scale bars, 1 mm. (C) PCR genotyping analyses of *E2f7* (top) and *E2f8* (bottom) using genomic DNA isolated from E10.5 placentas (Pla.) and fetuses (Fet.). Note that the *loxp* alleles were largely diminished and the *null* alleles could be readily observed in the *Cyp19-cre* placenta. Because the placenta is composed of extra-embryonic trophoblast cells as well as embryonic endothelial cells, the intact *loxp* alleles are likely from the fetal endothelial cell contamination. E10.5 $E2f7^{loxp/loxp}$;$E2f8^{loxp/loxp}$;$Rosa26^{loxp/loxp}$ (*control*) and *Cyp19-cre*;$E2f7^{loxp/loxp}$;$E2f8^{loxp/loxp}$;$Rosa26^{loxp/loxp}$ (*Cyp19-cre*) fetus and placenta sections were stained with X-gal and counterstained with nuclear fast red. Scale bars, 100 µm. Embryo cartoons at the top of the panels represent fetuses and placentas with wild type (black) or double mutant (white) genotypes.

Figure 6

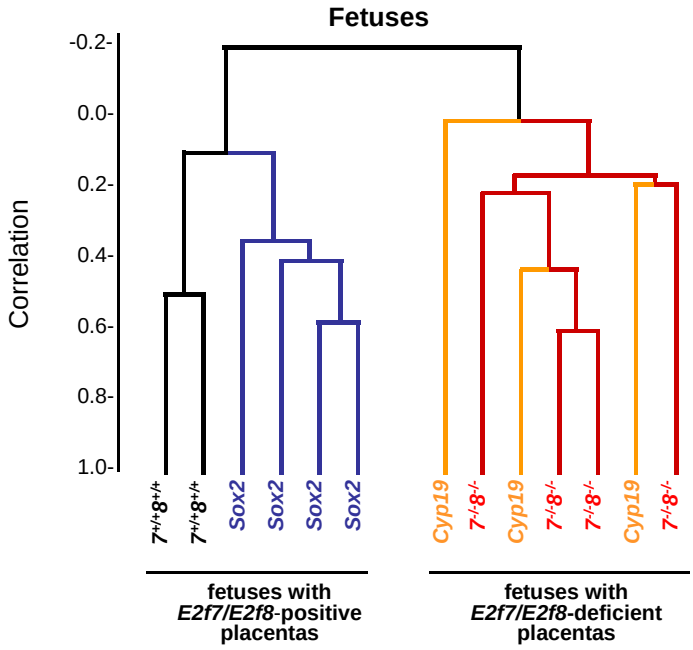

Loss of *E2f7* and *E2f8* in the Placenta Dictates Molecular Events in the Fetus
Dendogram of unsupervised clustering analysis using centered correlation and average linkage. E10.5 fetuses with the indicated genotypes were presented individually. Note the segregation of these fetuses based on the genotypes of their associated placentas.

Figure 7

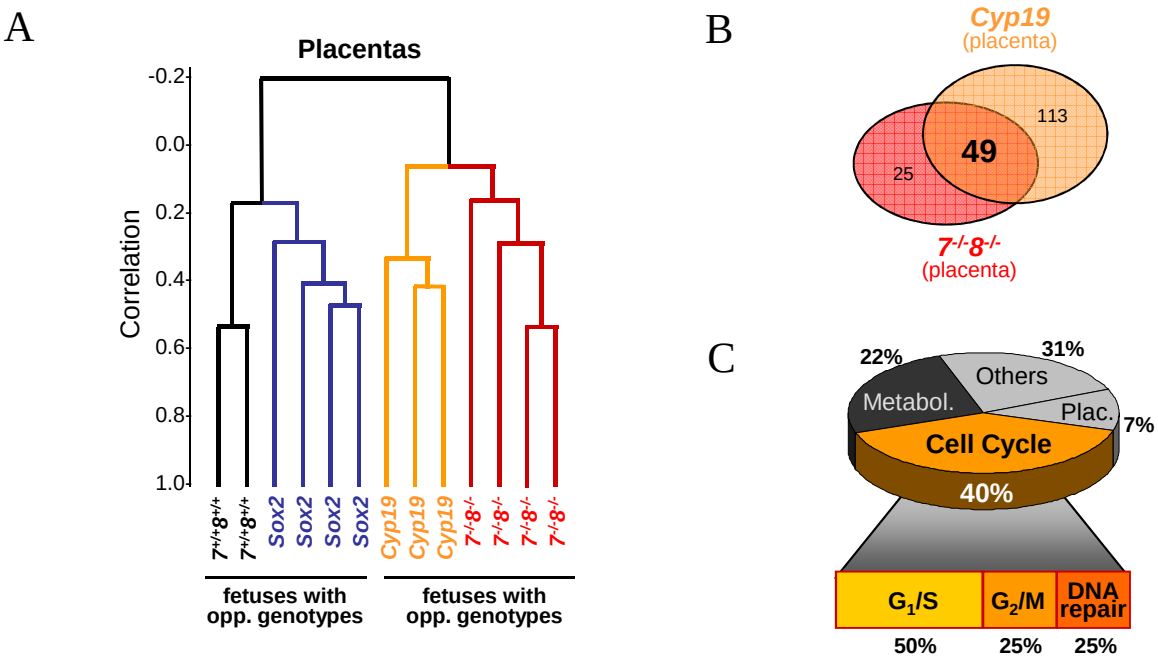

E2F7/E2F8-dependent Gene Expression in the Placenta. (A) Dendogram of unsupervised clustering analysis using centered correlation and average linkage. E10.5 placentas with the indicated genotypes were presented individually. Note the segregation of these placentas based on their genotypes. (B) Potential direct targets of E2F7 and E2F8 in placenta are presented by a two-set Venn diagram. Genes differentially upregulated in *E2f7*$^{-/-}$ *;E2f8*$^{-/-}$ and *Cyp19-cre* placentas with >2-fold (p<0.05) (C) Pie chart describing major gene ontology categories of 49 differentially expressed genes shown in Figure 7B

Figure 8

A

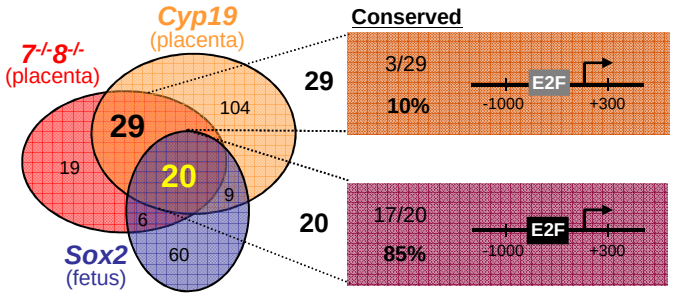

B

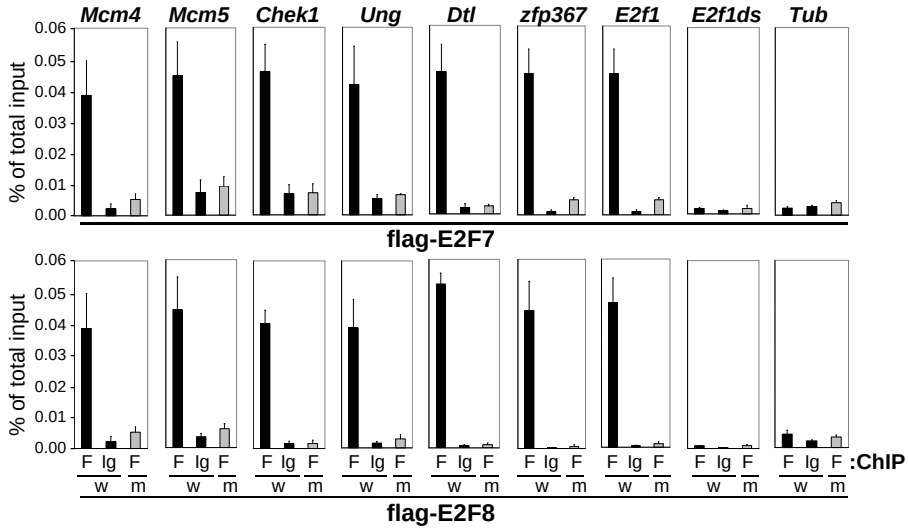

Identification of E2F7/E2F8 direct targets (A)) Left: potential E2F7 and E2F8 direct targets are presented by a three-set Venn diagram. Genes differentially upregulated in *E2f7-/-;E2f8-/-* and *Cyp19-cre* placentas with >2-fold (p<0.05) and in *Sox2-cre* fetuses with >1.6-fold (p<0.05) are shown as colored circles. Note that the overlapping area of all data sets contains 20 genes which are upregulated in a cell type-independent manner. Other 29 genes (26 annotated and 3 non-annotated) overlapped by only *E2f7-/-;E2f8-/-* and *Cyp19-cre* data sets are upregulated in a placenta-specific manner. Right: promoter analysis of the groups of 20 and 29 genes. The defined mouse and human promoter regions (-1000bp ~ +300bp) were examined for consensus E2F binding sites. Results are represented as a fraction and a percentage of genes that have at least one E2F binding site conserved between mice and humans (Conserved). (B)) Confirmation of promoter occupancy by E2F7 and E2F8 in HEK293 cells overexpressing flag-tagged E2F7 or E2F8 wild type (w), flag-tagged E2F7 or E2F8 DNA binding mutant (m) using a standard ChIP protocol. Normal mouse IgG was used as a negative control. Immunoprecipitates were amplified with primers specific to the E2F binding sites in promoters of the indicated genes, irrelevant sequences in the *tubulin* promoter (*Tub*) and in the *E2f1* coding region (*E2f1ds*). Real-time PCR was performed in triplicate and cycle numbers were normalized to 1% of the input. Error bars represent standard deviations.

Figure 9

20 potential direct targets of E2F7 and E2F8

Gene symbol	Function	E2F sites (mouse)	E2F sites (human)	Conserved Sites
2810417H13Rik (Paf)	PCNA-associated factor (p15PAF), oncogene, DNA replication	3	3	2
Cdc6	DNA replication	3	2	2
Zfp367	unknown	3	2	2
Dtl (Cdt2)	G2/M checkpoint	2	2	2
E2f1	G1 to S progression, apoptosis	2	2	2
Mcm4	DNA replication, transcription	4	3	1
Uhrf1 (ICBP90)	DNA repair, ubiquitin cycle, cell cycle	4	4	1
Mcm5	DNA replication, transcription	3	2	1
2600005O03Rik (Dscc1)	defective in sister chromatid cohesion homolog, cell cycle, DNA replication	2	2	1
Fbxl20	ubiquitin cycle	2	2	1
Chek1	G2/M transition, DNA damamge, DNA repair, meiotic recombination	1	4	1
Mcm10	DNA replication, G2/M checkpoints,	1	3	1
Gins2	DNA replication	3	1	0
Mcm6	DNA replication, transcription	3	3	0
Bard1	transcription, cell cycle, DNA damage, DNA repair, apoptosis	2	1	0
Ccdc59	regulation of transcription, DNA-dependent	1	0	0
Tacstd1	defense response	1	2	0
Cdc45l	cell cycle, DNA replication, cell division	0	1	0
Asb7	intracellular signaling cascade?	0	1	0
Ung	DNA base-excision repair	0	3	0

20 Direct Targets of E2F7 and E2F8.

Classification of tissue non-specific, direct targets of E2F7 and E2F8. E2F sites indicates number of consensus E2F binding sites between -1000bp and 300bp (promoter region)

Figure 10

29 targets without E2F binding site

Gene symbol	Function	E2F sites (mouse)	E2F sites (human)	Conserved sites
Hells	chromatin silencing, centric heterochromatin formation, mitosis, apoptosis	2	3	2
Phf19	regulation of transcription	4	3	1
Fbxo2	ubiquitin cycle, proteolysis	3	1	0
Srd5a1	androgen biosynthesis	3	2	0
Ak3l1 /// LOC100047616	nucleobase, nucleoside, nucleotide and nucleic acid metabolism	2	2	0
Trpm5	ion transport	2	0	0
Cdkn1a (p21)	cell cycle etc.	1	0	0
Egln3	oxygen sensor, HIF-PH3	1	3	0
Elf5	ectoderm development, transcription, EST family	1	0	0
Plxnb2	positive regulation of axonogenesis	1	2	0
Pthlh	cell proliferation, cAMP metabolism, development	1	0	0
Slco5a1	transport activity	1	1	0
Timp1	cell proliferation, erythrocyte maturation (x-chromosome)	1	1	0
5830482F20Rik	unknown	0	0	0
Aplp1	regulation of translation, extracellular matrix organization and biogenesis	0	1	0
Ceacam1	neovascularization, cell adhesion	0	2	0
Dll4	activates Notch, angiogenesis	0	2	0
Ecm1	extracellular matrix, transport	0	0	0
Fasl	cell death	0	0	0
Ifi30	unknown	0	0	0
Irx1	transcription, development	0	3	0
Klk1b22 /// Klk1b9	proteolysis	0	0	0
LOC100040854 /// LOC100040861 /// OTTMUSG00000010207	unknown	0	n/a	0
Myh6	muscle contraction	0	1	0
Pfpl	invasive trophoblast giant cells	0	n/a	0
Rpgrip1	eye photoreceptor cell development, response to stimulus	0	0	0
BC062258	could not find	n/a	n/a	n/a
D13Ertd608e	could not find	n/a	n/a	n/a
EG627488 /// EG667692 /// EG667695 /// LOC100043292	could not find	n/a	n/a	n/a

29 Placenta-Specific Targets of E2F7 and E2F8.

Classification of placenta-specific targets of E2F7 and E2F8. E2F sites indicates number of consensus E2F binding sites between -1000bp and 300bp (promoter region)

Figure 11

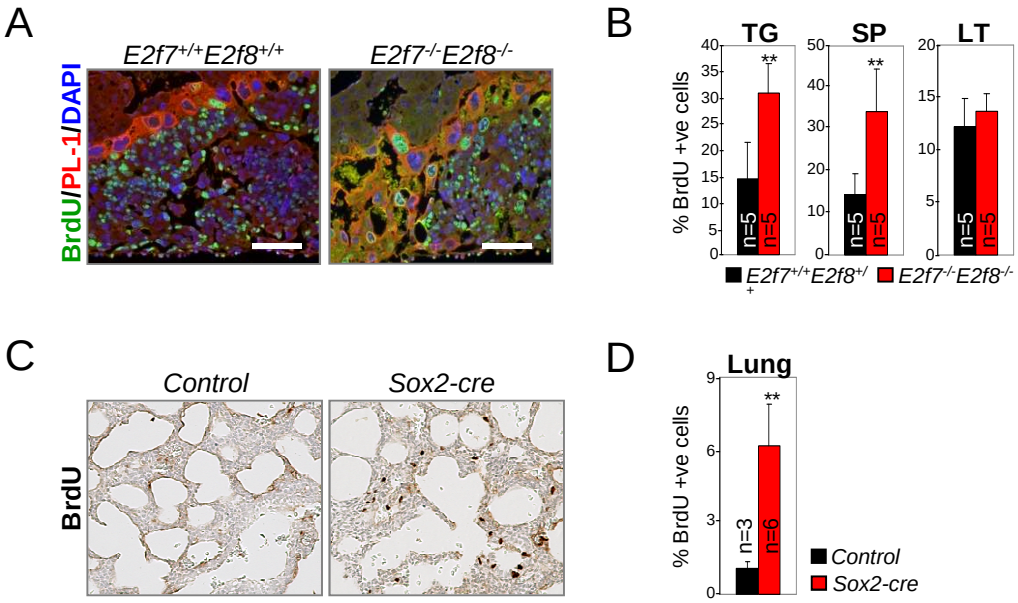

Deletion of *E2f7/E2f8* leads to ectopic DNA synthesis (A)Left: Merge images of immunofluorescence BrdU/PL-1 double staining on E10.5 placenta. Scale bars, 100 μm. (B) Percentages of BrdU positive cells were quantified for the indicated trophoblast cell types (TG, trophoblast giant cells; SP, spongiotrophoblasts; LT, labyrinth trophoblasts). Data are represented as the average ± SD percentage of positive cells. n, number of placenta samples analyzed for each genetic group Pairwise comparisons were evaluated by two-tailed Student's *t*-tests (** $p<0.006$). (C)) Immunohistochemistry using antibodies specific against BrdU in P0 lung. (D) Percentages of BrdU positive cells were quantified. Percentages were analyzed and compared as described above

Figure 12

A

Table: Genotypic analysis of embryos during development: *E2f3a/E2f7/E2f8* crosses

	E2F3a$^{+/+}$ *E2f7*$^{-/-}$*E2f8*$^{-/-}$	*E2f3a*$^{+/-}$ *E2f7*$^{-/-}$*E2f8*$^{-/-}$	*E2f3a*$^{-/-}$ *E2f7*$^{-/-}$*E2f8*$^{-/-}$	total
E10.5	-	9	23(1)	118
expected	-	*10*	*20*	
E14.5	-	-	6(2)[a]	57
expected	-	-	*10*	
P0	-	0	2(1)	37
expected	-	3	5	

() number of dead embryos; Exact binomial test: [a] highly significant ($p<0.0007$)

B

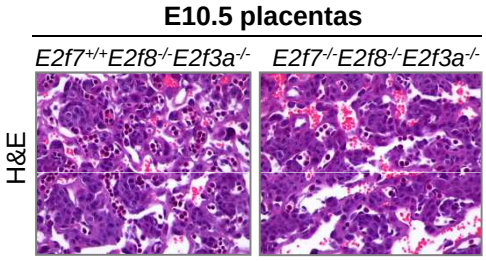

C

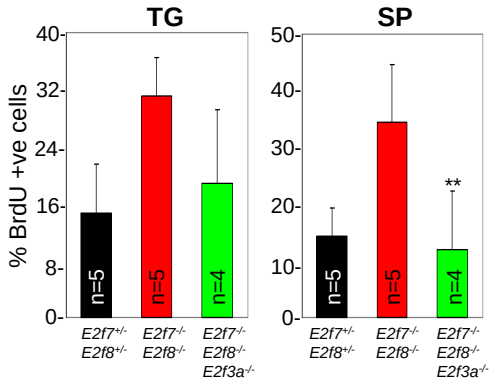

Loss of *E2f3a* rescues embryonic lethality in *E2f7/E2f8* double mutant embryos (A) Genotypic analysis of embryos derived from the *E2f3a/E2f7/E2f8* crosses at the indicated stages of development. (B) H&E staining of E10.5 placentas with the indicated genotypes. Note that the triple knockout placenta bears a high resemblance to the wild type placenta (C) Percentages of BrdU and P-H3 positive cells were quantified for the indicated trophoblast cell types (TG, trophoblast giant cells; SP, spongiotrophoblasts) in E10.5 placentas. Data are represented as the average ± SD percentage of positive cells. n, number of placenta samples analyzed for each genetic group Pairwise comparisons were evaluated by two-tailed Student's *t*-tests (** $p<0.006$).

Figure 13

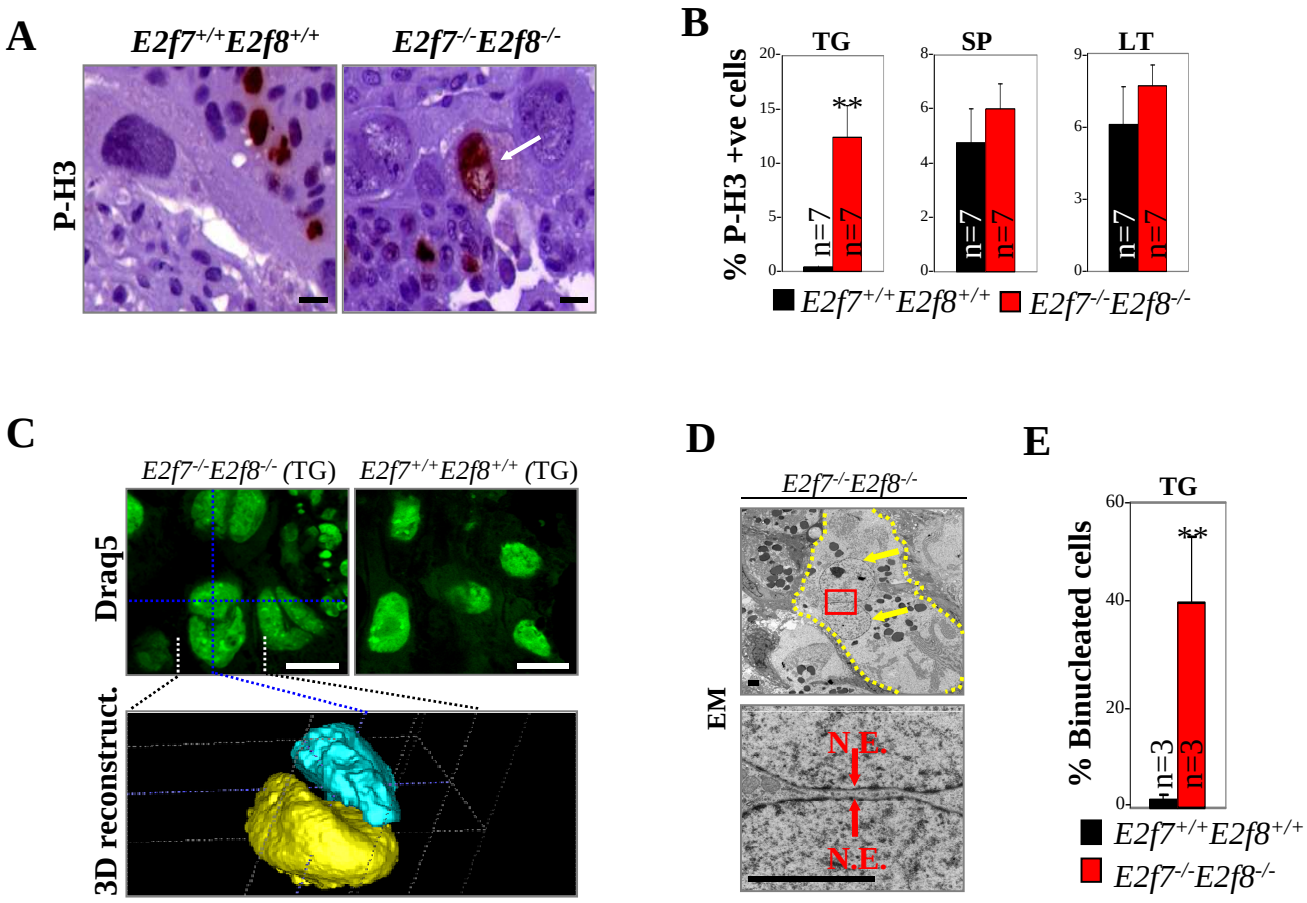

Loss of *E2f7/E2f8* Results in Aberrant Mitosis in Trophoblast Giant Cells

(A) Immunohistochemistry using antibodies specific against Phospho-Histone 3 on E10.5 placenta sections with the indicated genotypes. Positive trophoblast giant cells are indicated by arrows (B) Percentages of P-H3 positive cells were quantified for the indicated trophoblast cell types (TG, trophoblast giant cells; SP, spongiotrophoblasts; LT, labyrinth trophoblast) in E10.5 placentas. Data are represented as the average ± SD percentage of positive cells. n, number of placenta samples analyzed for each genetic group Pairwise comparisons were evaluated by two-tailed Student's *t*-tests (** $p<0.006$). (C) Top Panels: Draq5 Immunoflourescent staining of E10.5 placenta. Scale Bars, 100µm. Bottom Panel: 3D rendering of *E2f7*$^{-/-}$*E2f8*$^{-/-}$ Giant Cell. Each color represents distinct nucleus. Notice close proximity and tight fit, indicating recent karyokinesis. (D) Scanning Electron Microscopic image of *E2f7*$^{-/-}$*E2f8*$^{-/-}$ E10.5 placenta. Top Panel: Dotted line marks cell membrane. Distinct nuclei are indicated by arrows. Bottom Panel: close up view of top panel. N.E., nuclear envelope. Notice two distinct nuclei within one cell membrane. (E) Percentages of binuclead cells were quantified for trophoblast giant cells (TG) in E10.5 placentas. Data are represented as the average ± SD percentage of binucleated cells. n, number of placenta samples analyzed for each genetic group Pairwise comparisons were evaluated by two-tailed Student's *t*-tests (** $p<0.006$).

Figure 14

A

Genotypic analysis of embryos during development: *Rb/p107* crosses

	$Rb^{+/+}$			$Rb^{+/-}$			$Rb^{-/-}$			total
	$p107^{+/+}$	$p107^{+/-}$	$p107^{-/-}$	$p107^{+/+}$	$p107^{+/-}$	$p107^{-/-}$	$p107^{+/+}$	$p107^{+/-}$	$p107^{-/-}$	
E10.5	2	9	4	10	18(7)	13	4	12	7(2)	88
expected	*6*	*11*	*6*	*11*	*22*	*11*	*6*	*11*	*6*	
E11.5	1	1	2(1)	1(1)	3	4	3	1	0	18
expected	*1*	*2*	*1*	*2*	*4*	*2*	*1*	*2*	*1*	

() number of dead embryos recovered; Exact binomial test: [a] significant (p=0.0015), [b] highly significant (p<0.0007).

B

Genotypic analysis of embryos during development: *Rb-p130*

	$Rb^{+/+}$			$Rb^{+/-}$			$Rb^{-/-}$			total
	$p130^{+/+}$	$p130^{+/-}$	$p130^{-/-}$	$p130^{+/+}$	$p130^{+/-}$	$p130^{-/-}$	$p130^{+/+}$	$p130^{+/-}$	$p130^{-/-}$	
E12.5	4(1)	9	7	5	29(2)	16(3)	2(1)	9(5)	3(2)	98
expected	*6*	*12*	*7*	*11*	*25*	*14*	*6*	*12*	*7*	
E13.5	6(1)	16	0	18(2)	27	7	5(3)	4(8)	3(4)	105
expected	*7*	*13*	*7*	*13*	*26*	*13*	*7*	*13*	*7*	

() number of dead embryos recovered; Exact binomial test: [a] significant (p=xxxxx), [b] highly significant (p<xxxxx).

Knockout of *Rb/p107* recapitulates the *E2f7/E2f8* lethality timepoint (A) Genotypic analysis of embryos derived from the *Rb/p107* crosses at the indicated stages of development. (B) Genotypic analysis of embryos derived from the *Rb/p130* crosses at the indicated stages of development

Figure 15

Genotypic analysis of embryos during development: *E2f7/E2f8/Rb/p107* crosses

	E2f7$^{+/-}$*E2f8*$^{+/-}$	*E2f7*$^{-/-}$*E2f8*$^{+/-}$		*E2f7*$^{+/-}$*E2f8*$^{-/-}$		total
	Rb$^{+/-}$*p107*$^{+/-}$	*Rb*$^{+/+}$*p107*$^{+/-}$	*Rb*$^{+/-}$*p107*$^{+/-}$	*Rb*$^{+/+}$*p107*$^{+/-}$	*Rb*$^{+/-}$*p107*$^{+/-}$	
P0	7(1)	6	5	4(1)	1(1)	121
expected	*6*	*4*	*4*	*5*	*5*	
P21	20	7	1	9	1	230
expected	*15*	*6*	*6*	*7*	*7*	

() number of dead embryos; Exact binomial test: [a] highly significant ($p < 0.0001$).

E2f7/E2f8 share a prominent genetic interaction with Rb/p107. Genotypic analysis of embryos derived from the *E2f7/E2f8/Rb/p107* crosses at the indicated stages of development